Hindawi
Journal of Nanomaterials
Volume 2017, Article ID 6298307, 14 pages
https://doi.org/10.1155/2017/6298307

Research Article

TiO_2 (Nano)Particles Extracted from Sugar-Coated Confectionery

Martina Lorenzetti,[1] Anja Drame,[1,2] Sašo Šturm,[1] and Saša Novak[1,2]

[1]*Department for Nanostructured Materials, Jožef Stefan Institute, Jamova Cesta 39, SI-1000 Ljubljana, Slovenia*
[2]*Jožef Stefan International Postgraduate School, Jamova Cesta 39, SI-1000 Ljubljana, Slovenia*

Correspondence should be addressed to Martina Lorenzetti; martina.lorenzetti@ijs.si

Received 4 October 2016; Accepted 15 November 2016; Published 3 April 2017

Academic Editor: Ilaria Fratoddi

As the debate about TiO_2 food additive safety is still open, the present study focuses on the extraction and characterisation of TiO_2 (nano)particles added as a whitening agent to confectionary products, that is, chewing gum pellets. The aim was to (1) determine the colloidal properties of suspensions mutually containing TiO_2 and all other chewing gum ingredients in biologically relevant media (preingestion conditions); (2) characterise the TiO_2 (nano)particles extracted from the chewing gum coating (after ingestion); and (3) verify their potential photocatalysis. The particle size distribution, in agreement with the zeta potential results, indicated that a small but significant portion of the particle population retained mean dimensions close to the nanosize range, even in conditions of moderate stability, and in presence of all other ingredients. The dispersibility was enhanced by proteins (i.e., albumin), which acted as surfactants and reduced particle size. The particle extraction methods involved conventional techniques and no harmful chemicals. The presence of TiO_2 particles embedded in the sugar-based coating was confirmed, including 17–30% fraction in the nanorange (<100 nm). The decomposition of organics under UV irradiation proved the photocatalytic activity of the extracted (nano)particles. Surprisingly, photocatalysis occurred even in presence of an amorphous SiO_2 layer surrounding the TiO_2 particles.

1. Introduction

In the last few years industrially processed food products have been increasingly supplemented with various additives, such as colours, flavours, thickening, and anticaking agents during the food preparation. Among the allowed additives in Europe [1], titanium dioxide (TiO_2) is one of the most widely used. Classified as food-grade white pigment (E171) [2], TiO_2 powder is part of the "Group II: Food colours authorised at *quantum satis*" according to the European legislation [3], while its amount is limited to 1% by weight of food according to the US Food and Drug Administration (FDA) authority [4].

At the same time, with the advent of nanotechnologies, consumers have been progressively more exposed to nanoparticles (NPs) from different sources, that is, pharmaceutical products (drugs), cleaning agents in sprays, and paints, and also from the food chain. Even though not intentionally produced as nanomaterials, food additives can contain quite large fraction of particles in the nanosized range, increasing the daily exposures of consumers to NPs. According to the European Commission [5] a material is defined as nanomaterial if 50% or more of particles have a size between 1 nm and 100 nm. In case of titanium dioxide, a recent study [6] reported that approximately 36% of TiO_2 particles extracted from food products available on the US market owned at least one dimension in the nano range. The rising daily exposure to nanoparticles and intake via ingestion, inhalation, skin adsorption, and so on may result in cumulative high doses in the human body, which is hard to predict and control on the long term, that is, in a few years. Taken together, all these results have been generating lots of concerns within the biomedical community about (nano)TiO_2 safety.

The determination of the NPs presence in food and their physicochemical characteristics represent the initial, fundamental step before any risk assessment study is performed. The identification of TiO_2 (nano)particles intentionally added to confectionery food was chosen as the main task of this research work. Among the sugar-coated confectionery

products, chewing gums are in the top 20 products in terms of Ti concentration, with a Ti content greater than 0.12 μg/mg [6]. Due to these remarkable findings, together with the easy availability and spread consumption (children and adults), sugar-coated chewing gums were chosen as representative food samples containing TiO_2 (nano)particles. As described in the Scientific Opinion document edited by the European Food Safety Authority (EFSA) about the application of nanotechnologies in the food chain [7], the risk of a nanomaterial depends on its chemical composition, physicochemical properties, interactions with tissues, and potential exposure levels. Among the parameters considered for the nanoparticles characterisation, EFSA identifies the chemical composition, particle size, morphology, surface charge, and pH as essential for either dry powders or dispersions [7]. When dealing with complex matrices as food, the behaviour of a single component (i.e., NPs) has to be interpreted also on the basis of additional interactions with ions, amino acids, and proteins contained in the body juices. Accordingly, the properties of the sugar-based chewing gum coatings were studied by considering the whole scraped triturate, thus composed of TiO_2 particles together with the other gum ingredients. Besides the chemical composition and microscopical appearance, it is known that not only size in the dry state but also surface charge influences the cellular uptake of nanoparticles [8] and that the oral uptake occurs already in the oral cavity [9]. For the first time we carried out a systematic study on the dispersibility, size distribution, and surface charge of TiO_2 particles embedded within other coating ingredients by preparing suspensions in biologically relevant fluids. This allowed mimicking the real conditions of the particles in the oral cavity during consumption, as well as their status in various body compartments. For completeness, TiO_2 particles were also extracted from the sugar-based matrix via dissolution, separation, and purification by slightly modifying three simple methods described in literature. During the particle extraction, the main goal was to avoid the use of any hazardous or environmentally risky chemical (e.g., strong acids) and overcome the application of complex analytical methods such as inductively coupled plasma or field flow fractionation. The extracted powders in their dry state were characterised to verify the physicochemical stability of the particles, especially in terms of their capability to form reactive oxygen species (ROS), which might negatively interact with cells and tissues.

The results obtained from this work on the characteristics of the sugar-based coatings for confectionery and the investigation of their suspensions properties are applicable to other food products containing TiO_2 (nano)particles. Therefore, this study is expected to give important, basic information to researchers involved into biological analyses for risk assessment.

2. Materials and Methods

In this study, five types of sugar-coated chewing gums (referred to hereinafter as gums A, B, C, D, and E), in the form of pellets, were randomly selected among the brands commonly available on the market in 2015 with declared

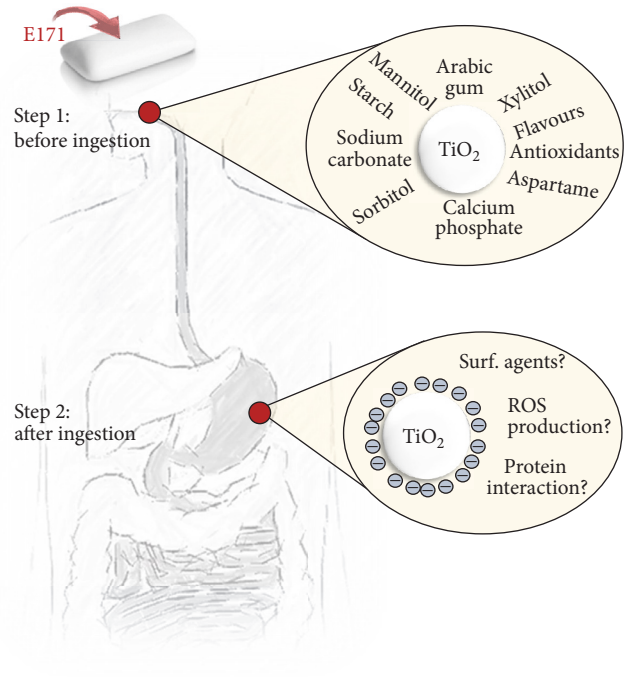

Figure 1: Experimental concept scheme.

"titanium dioxide," "TiO_2," or "E171" on the ingredient label, but without any indication of nanosized ingredients.

As reported in [6], more than 90% of TiO_2 was associated with the outer shell of chewing gums. Therefore, the extraction and identification of TiO_2 (nano)particles were performed only from the sugar-based coatings.

A scheme of the experimental concept of this study is presented in Figure 1. The first stage ("Step 1") was based on the characterisation of "as-scraped" coatings to assess the physicochemical behaviour of TiO_2 particles as present in the chewing gum coating matrix; "Step 1" was meant to mimic the condition of the particles before ingestion, namely, being still embedded within the chewing coating, and before any extraction, cleaning, or further manipulation. The second step concerned the characterisation of the particles after their extraction from the food matrix (after ingestion and partial digestion).

2.1. Physicochemical Characterisation. The physicochemical characterisation was carried out on both the "scraped" coatings (TiO_2 particles together with all the other components studied as colloids) in "Step 1" and the extracted particles by Methods 1, 2, and 3 in Step 2. This approach aimed at mimicking the particles conditions before ("Step 1," "scraped" coatings) and after their ingestion ("Step 2," extracted particles), respectively. For comparison, a food-grade E171 powder (hereinafter FG-ref), purchased on the web as composed of pure TiO_2 (Super Duper White icing whitener buttercream colouring superwhite cupcakes, Cake Stuff), was used in this study as reference material.

2.1.1. Colloidal Properties of the Particles: Surface Charge and Particle Size Distribution. In "Step 1," the colloidal properties

of the TiO_2 particles overlaid by the sugar-based matrix were analyzed in suspension. The solvents for the suspensions, chosen for their biological relevance, were as follows: ultra-pure water, Fusayama and Mayer artificial saliva (AS) prepared according to [10] (pH = 5.3–5.9), 0.1 M phosphate buffer saline solution (PBS, tablets, Sigma Aldrich) (pH = 7.47), and Dulbecco's Modified Eagle Medium for cell cultures (DMEM 1x with Glutamax-I, 1 g/L D-Glucose, pyruvate, Gibco, Life Technologies) used as received (DMEM 1 : 1, pH = 7.47) or diluted 100 times in ultra-pure water (DMEM 1 : 100, pH = 7.15). All the obtained suspensions were stirred for 5 min prior any analysis.

The zeta potential (ZP) of 0.5 w/v% suspensions in all the abovementioned solvents at inherent pH was evaluated by the Dynamic or Phase Analysis Light Scattering system (PALS, ZetaPALS Potential Analyzer, Brookhaven Instruments Ltd.) based on the electrophoretic mobility principle. The Smoluchowski model was applied for the ZP calculations. The reference suspensions containing FG-ref powder were prepared at 0.005 w/v% concentration (100 times lower than the chewing gum samples) by considering that the gum coatings could contain an amount of TiO_2 up to 1 w/w% of the coating mass.

The Multiangle Particle Sizing option (scattering angle 90°, beam wavelength 658 nm, run time 1 min, and 90Plus/BIMAS, Brookhaven Instruments Ltd.) available on the ZetaPALS instrument allowed the assessment of the polydispersity index (PDI) and the effective/hydrodynamic particle diameter (D_{eff}) in all the abovementioned solvents.

The influence of protein corona on the particles D_{eff} was assessed by using bovine serum albumin (BSA, Sigma Aldrich) as a protein model [11]. Firstly, a stock solution of 0.5 w/v% particle suspension (chewing gum E scraped coating) and 0.005 w/v% (FG-ref powder) was prepared in ultrapure water and stirred for 5 min; then, 0.075 mL BSA (with increasing concentrations up to 1.5 mg/mL) was admixed to 2.425 mL stock solution and stirred for 1 min; lastly, 0.25 mL of PBS 10x solution was added (final PBS concentration: 1x) and stirred for 1 min, before the analysis of D_{eff}.

The particle size distribution was also evaluated by dynamic laser diffraction (LD) based on the Mie scattering principle (LA-920 particle size analyzer equipped with He-Ne laser, wavelength 632.8 nm, Horiba); the data are reported as the log-normal mean value and/or the mean values of each of the two peaks in case of bimodal distributions.

2.1.2. Morphology, Primary Particle Size, and Crystallinity. In "Step 2," the investigations of the TiO_2 nanoparticles morphology, crystal structure, and composition were performed by field emission scanning electron microscopy (FE-SEM, JEOL JSM 7600F, Japan) and by an aberration-corrected probe TEM (JEOL JEM-ARM200F), using the cold field emission source and equipped with energy Dispersive X-ray Spectroscopy (EDXS) system (Centurio 100 mm^2, JEOL). The probe size for Scanning TEM (STEM) imaging was set to 0.1 nm, with a current of 20 pA and the convergence semiangle of 24 mrad. STEM images were acquired in a so-called High-Angle Annular Dark-Field (HAADF) mode. The EDXS spectrum images were performed with the probe size of 0.2 nm, under continuous scanning mode with a pixel dwell time of 25 microseconds and by using probe currents of 250 pA. The primary particle size was quantitatively estimated from the SEM micrographs by SMileView software (version 2.725, JEOL Ltd.). Five different micrographs per sample were chosen and a total of 250–400 particles were measured for statistics.

The crystal phases were analyzed by X-ray diffractometry (Siemens D5000, Germany) using a CuKα1 radiation (1.5406 Å) within a range of 2θ angle scanned from 10° to 70°. The diffractograms were interpreted by using X'Pert HighScore software (version 2.1.2).

The mass of the extracted TiO_2 particles was normalised to the total mass of the pellet (Method 3), in order to calculate the TiO_2 content.

2.2. Organics Degradation via TiO_2 Photocatalysis. In "Step 2," the evaluation of the catalytic activity of the extracted TiO_2 particles was assessed by photoinduced decomposition of caffeine (≥99.0% HPLC grade, Sigma-Aldrich Chemie GmbH, Steinheim), used as representative organic molecule [12]. Suspensions of extracted TiO_2 particles by Method 3 (0.05 w/v% and 0.005 w/v%) in caffeine solution (10 ppm) were irradiated under stirring using a UV-vis simulated sun spectrum (Osram UV bulbs without UVC, Ultra Vitalux) up to 4 h. The suspensions were sampled at different times, then the collected fractions were centrifuged for 5 min at 13,400 rpm (MiniSpin Centrifuge, Eppendorf), and the intensity of absorption of the supernatants was analyzed by spectrophotometer (Lambda 950 UV/Vis/NIR, PerkinElmer). FG-ref powder was used as reference material.

2.3. Extraction of Particles out of the Chewing Gum Coating. The samples for "Step 2" were obtained by extracting the TiO_2 particles from the "scraped" external coating or directly from the "as-produced" pellets, resulting in three different extraction methods, as summarised in Figure 2. The dissolution step served to dissolved the soluble components, while the purification step in combination with the separation allowed for the removal of other food additives [13].

Method 1. Four pellets per chewing gum type were scraped and the collected powder (0.7–1 g) was admixed with 30 mL of ultrapure water (Labostar TWF-UV7, Siemens). The suspension was ultrasonicated for 10 min to dissolve the soluble coating ingredients from the TiO_2 particles and detach the other insoluble components. The suspension was then centrifuged at 13000 g for 15 min (model number 5804, Eppendorf, equipped with a fixed-angle rotor). The obtained precipitate at the bottom of tube was washed with other 30 mL of water; the procedure was repeated for a total of 4 times. Method 1 was designed by modifying the procedure used in [14].

Method 2. Four pellets per chewing gum type were scraped and the collected powder (0.7–1 g) was admixed with 30 mL of ultrapure water. The suspension was ultrasonicated for 10 min and then centrifuged at 13000 g for 15 min. The

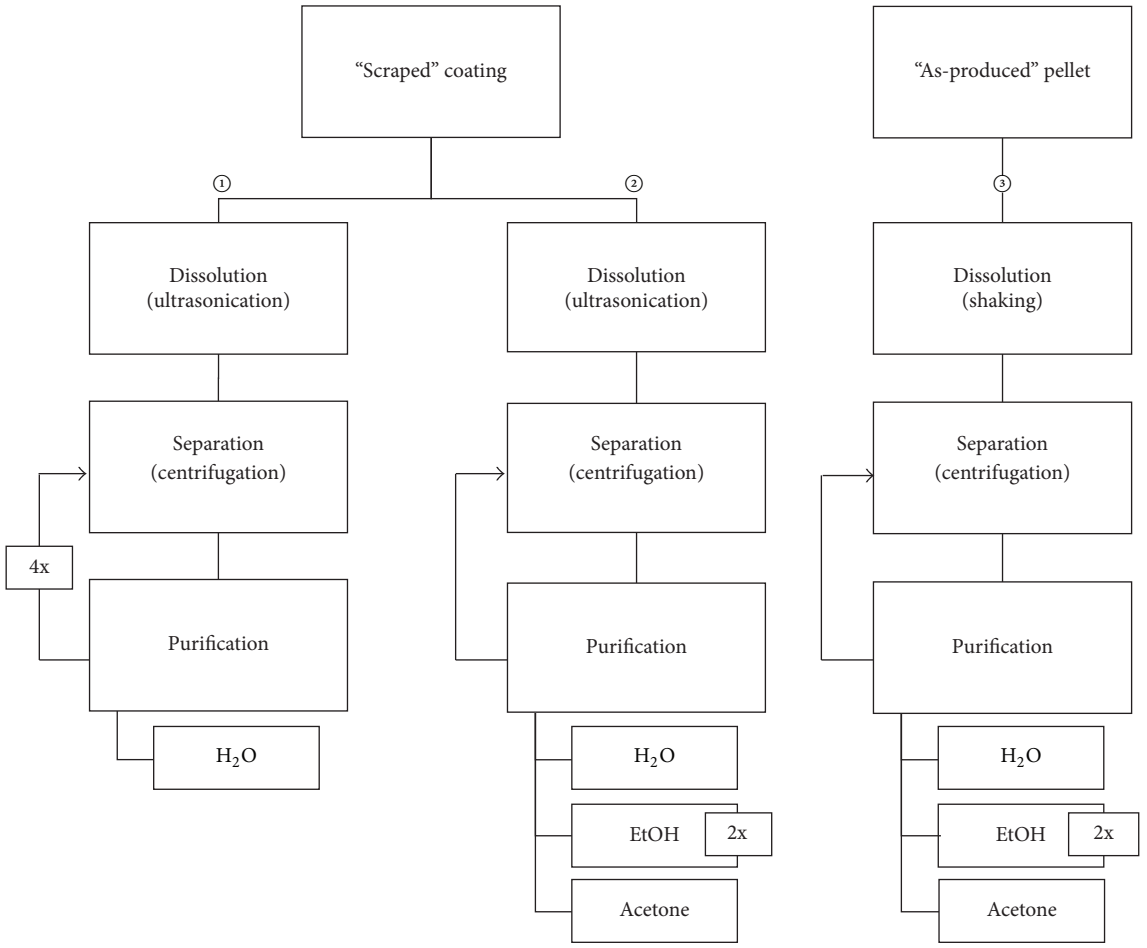

Figure 2: Scheme of TiO_2 particles extraction.

obtained precipitate at the bottom of tube was washed consecutively with solvents at different polarities to improve the cleaning of the particles. Accordingly, 20 mL of ultrapure water, acetone (2 times), and absolute ethanol were added in sequence to the precipitate before each centrifugation step (3200 g for 15 min). Method 2 was designed by modifying the procedure used in [13].

Method 3. The sugar-based coating was dissolved directly from the chewing gum pellet. Each pellet was immerged in a tube containing 7.5 mL of ultrapure water. The tube was gently shaken for 5 min at 80 rpm at 25°C (KS 3000 i control, IKA). The pellet was moved in another tube containing 5 mL of ultrapure water and the shaking was repeated. Both suspensions obtained by dissolution were collected and centrifuged at 12000 g for 15 min. The obtained precipitate was washed consecutively with 10 mL of ultrapure water, acetone (2 times), and absolute ethanol and recentrifuged at 12000 g for 15 min each cycle. Method 3 repeated the procedure used in [13].

Finally, the precipitate obtained by any extraction method was dried in vacuum drier (Heraeus vacutherm, series 6000, Pfeiffer vacuum) at 70°C for 1.5 h and weighted for obtaining the extracted mass.

3. Results

3.1. Step 1: Colloidal Properties of "As-Scraped" Coatings. In order to perform the characterisation in Step 1, the chewing gum coatings were firstly "scraped," then smashed as powder, and lastly dispersed in biologically relevant fluids. The properties of the "scraped" coatings (composed of TiO_2 particles together with the other gum ingredients) were characterised by analyzing the colloidal suspension of the scraped particles in terms of inherent pH, surface charge, and particle size distribution.

3.1.1. Inherent pH. The inherent pH values of the obtained suspensions are reported in Table 1. All the scraped coatings tended to basic pH in water (pH between 7.2 and 9.2), while pure TiO_2 (FG-ref) was slightly acidic (pH 6.6). The pH of the suspensions rose in artificial saliva (AS) and diluted DMEM 1 : 100 in comparison to the starting pH of the solvents (5.3–5.9 and 7.2, resp.), but it was kept almost constant at physiological values for the buffered PBS and DMEM 1 : 1.

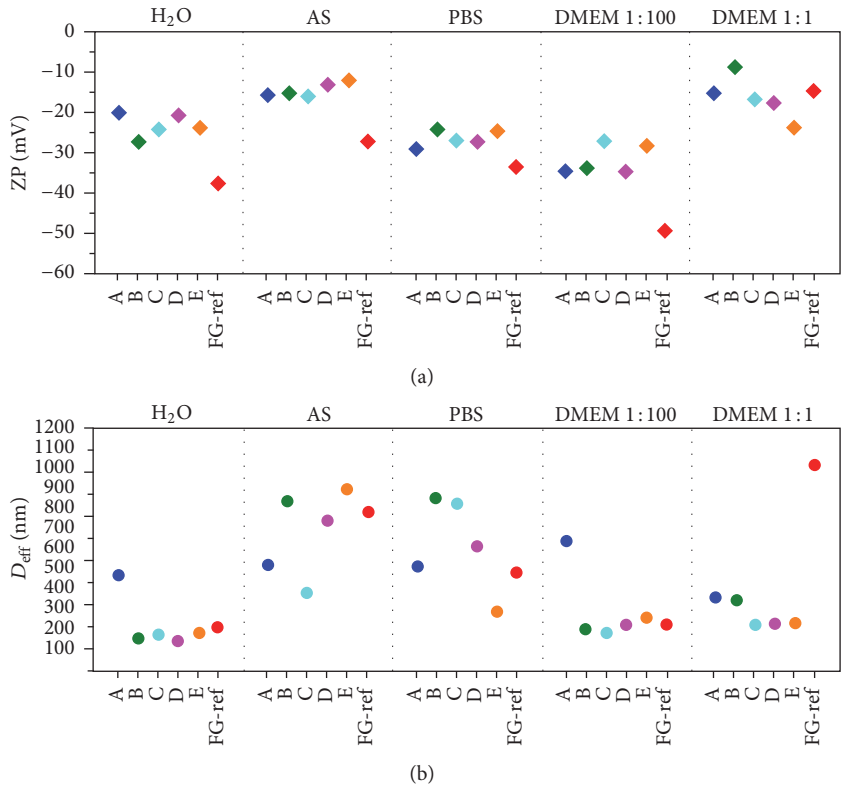

Figure 3: (a) Surface charge, expressed as zeta potential (ZP), and (b) effective diameter (D_{eff}) of "scraped" coatings from chewing gums A–E and FG-ref powder in different fluids: ultrapure water (H_2O), artificial saliva (AS), phosphate buffered saline solution (PBS), and Dulbecco's Modified Eagle Medium for cell cultures (diluted: DMEM 1 : 100; concentrated: DMEM 1 : 1).

Table 1: Inherent pH values of chewing gums A–E and E171 powder in different fluids: ultrapure water (H_2O), artificial saliva (AS), phosphate buffered saline solution (PBS), Dulbecco's Modified Eagle Medium for cell cultures (diluted: DMEM 1 : 100; concentrated: DMEM 1 : 1).

Sample	pH				
	H_2O	AS	PBS	DMEM 1 : 100	DMEM 1 : 1
A	8.8	6.1	7.3	8.7	7.5
B	9.0	7.2	6.9	8.8	8.1
C	8.5	6.9	7.5	8.3	7.5
D	7.2	6.7	7.1	7.7	8.2
E	7.3	7.6	7.2	7.7	7.5
E171	6.7	6.4	7.2	7.5	7.5

3.1.2. Surface Charge. The results on zeta potential in various liquids and the effective diameter of the chewing gum powders are summarised in Figure 3. All the powders scraped from chewing gum appeared negatively charged and, in most cases, there was no significant scatter within the ZP values in the same medium (Figure 3(a)). Only FG-ref represented an exception, showing a generally higher ZP magnitude than the "scraped" coatings, especially in water, artificial saliva, and DMEM 1 : 100. In comparison to the bare FG-ref powder, the ZP decreased in magnitude (around −25 mV) for the sugar-based "scraped" coatings (samples A–E) dispersed in water, as well as in PBS. A different behaviour was observed for the "scraped" coatings in artificial saliva and cell medium DMEM 1 : 1, in which the ZP dropped down to −10/−15 mV. Lastly, suspensions of samples A–E in DMEM 1 : 100 exhibited ZP values in the range of −30/−35 mV.

3.1.3. Particle Size Distribution. The particle effective diameter (D_{eff}) for the "scraped" coatings A–E was obtained by dynamic light scattering (DLS) analysis (Figure 3(b)). The particles in H_2O and in DMEM presented small D_{eff} values, followed by the ones dispersed in PBS and AS. For instance, in water the samples presented good dispersibility and the D_{eff} values of the agglomerates ranged between 200 and 300 nm (exception: chewing gum A). On the other hand, the "scraped" coatings A–E presented large scattering of data in case of physiological AS and PBS.

The DLS served also for monitoring the effect of bovine serum albumin (BSA) on the agglomeration of the scraped coatings. Figure 4 reports the D_{eff} for chewing gum E and for FG-ref (reference) at increasing BSA concentrations. Both samples revealed the same trend: the higher the BSA concentration was, the more their D_{eff} decreased till a minimum value, before D_{eff} started increasing again. Chewing gum E reached the maximal dispersibility (lowest D_{eff} = ~300 nm) with 0.20 mg/mL BSA, while FG-ref needed 1.00 mg/mL BSA to get its smallest D_{eff} = ~350 nm.

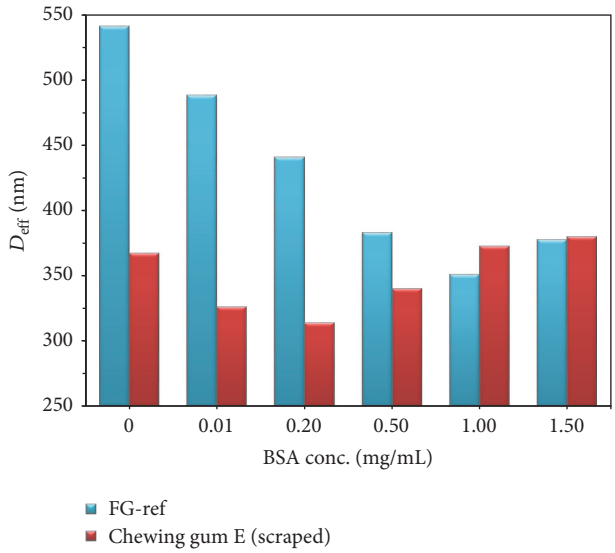

Figure 4: Hydrodynamic diameter (D_{eff}) as a function of protein (BSA) concentration for the scraped coating from chewing gum E and FG-ref powder.

Laser diffraction (LD) was used as a second technique for particle size analysis in wet conditions. In this case, the effect of the mechanical forces applied to the suspension was also considered. Figure 5 shows the particle size distribution for chewing gums A and E (chosen as examples), obtained by only stirring (mix), or after ultrasonication of the suspensions for different times, namely, for 5, 10, and 15 minutes (mix + US 5 min, mix + US 10 min, and mix + US 15 min). When only stirring was applied to the suspensions of "scraped" coatings, sample E displayed the narrowest particle size distribution and the lowest diameter in all the media (Figure 5, red dotted lines) among the five types of the examined chewing gums. As expected, sonication allows for higher dispersion of the particles and, possibly, a higher dissolution of the sugar-based coating, especially at longer sonication times (Figure 5, blue solid line). This contributed to separate the particle populations into two distinct peaks for bimodal distributions (i.e., sample A) and/or to narrow the distribution towards nanosized-range diameters (sample E) in comparison with the solely mixing.

3.2. Step 2: Analyses on the TiO_2 Extracted Particles

3.2.1. Morphology and Primary Particle Size. All the extracted particles appeared irregular shaped with rounded edges under scanning electron microscopy imaging, resembling the ones composing the FG-ref reference powder (data not shown). Figure 6 shows chosen samples (chewing gums A and E) after extraction by Methods 1, 2, and 3. The SEM micrographs for all the studied samples extracted by the three methods are collected in the Supplementary Materials file (Figures S1–3 in Supplementary Material available online at https://doi.org/10.1155/2017/6298307). From a qualitative viewpoint, the extracted particles from samples D and E appeared as the cleanest among the five types of analyzed chewing gums, regardless of the extraction process (Figures S1–3). Indeed, the TiO_2 particles from samples A, B, and C appeared by SEM still welded with big solids (Figures S1–3) composed of a mixture of organic/inorganic matrix that any extraction procedure was able to dissolve and caused blurry images at high magnification. Comparing the three methods, the extraction performed from the "scraped" coatings (Methods 1 and 2) was less effective than the one applied to the whole chewing gum pellet (Method 3). Accordingly, only the SEM images relative to the Method 3 extraction were used for the primary particle size calculations. All the samples showed a mean primary crystal size of ~130 nm (sample A: 147 ± 49 nm; sample B: 133 ± 46 nm; sample C: 142 ± 46 nm; sample D: 131 ± 42 nm; sample E: 128 ± 43 nm).

3.2.2. Crystalline Phase Composition. The XRD analysis was employed to verify the crystalline structure and the cleanness of the extracted particles. All the spectra showed single peaks at 25.3° and 48.1°, and the triple peak centred at $2\theta \sim 38°$, typical for the TiO_2-anatase crystalline structure (Figure 7(a)). These peaks appeared very intense and sharp in comparison to the diffractogram of "as-scraped" coatings (Figure 7(b)), which indicates the effectiveness of the extraction method to obtain clean particles (in agreement with the SEM results (Figure 6)).

Since the particles extracted by Method 3 from the chewing gum E (E-3) appeared as the cleanest, this sample was chosen for further analyses.

3.2.3. Chemical Composition and Mapping. A representative TEM image of TiO_2 nanoparticles from FG-ref and E-3 sample is shown in Figure 8(a). The majority of nanoparticles are found in aggregates, composed of a few to several dozen nanoparticles bonded together by well-defined grain boundaries. The individual nanoparticles are roundly shaped and of similar size, ranging between 50 nm and 200 nm. The selected area diffraction pattern (SAED) acquired from the area rich in TiO_2 matches perfectly with the anatase crystal structure (ICSD 92363). The detailed analysis of particle surfaces showed that the majority of TiO_2 particles are covered by a thin amorphous layer. The thickest amorphous layer of 20 nm was found on the FG-ref particles (Figure 8(b)), while it was discontinuous in the case of sample E-3, with an average thickness of 5 nm (Figure 8(c)). The energy dispersive X-ray (EDXS) elemental maps that were performed on the individual nanoparticles from sample E-3 revealed the enrichment of the amorphous surface layer by the element Si. That implies that the TiO_2 nanoparticles were coated with a thin layer of amorphous SiO_2, probably in their final stage of fabrication (Figure 8(d)).

3.2.4. TiO_2 Photocatalysis. The photocatalytic activity of FG-ref powder and TiO_2 particles extracted from sample E-3 was revealed by the degradation of caffeine (10 ppm) under irradiation. Both powders underwent photocatalysis, regardless of their concentration in suspension (Figure 9). The complete caffeine degradation occurred in 1 h in case of 0.05 w/v% TiO_2 concentration, while it took 2 h and 4 h in

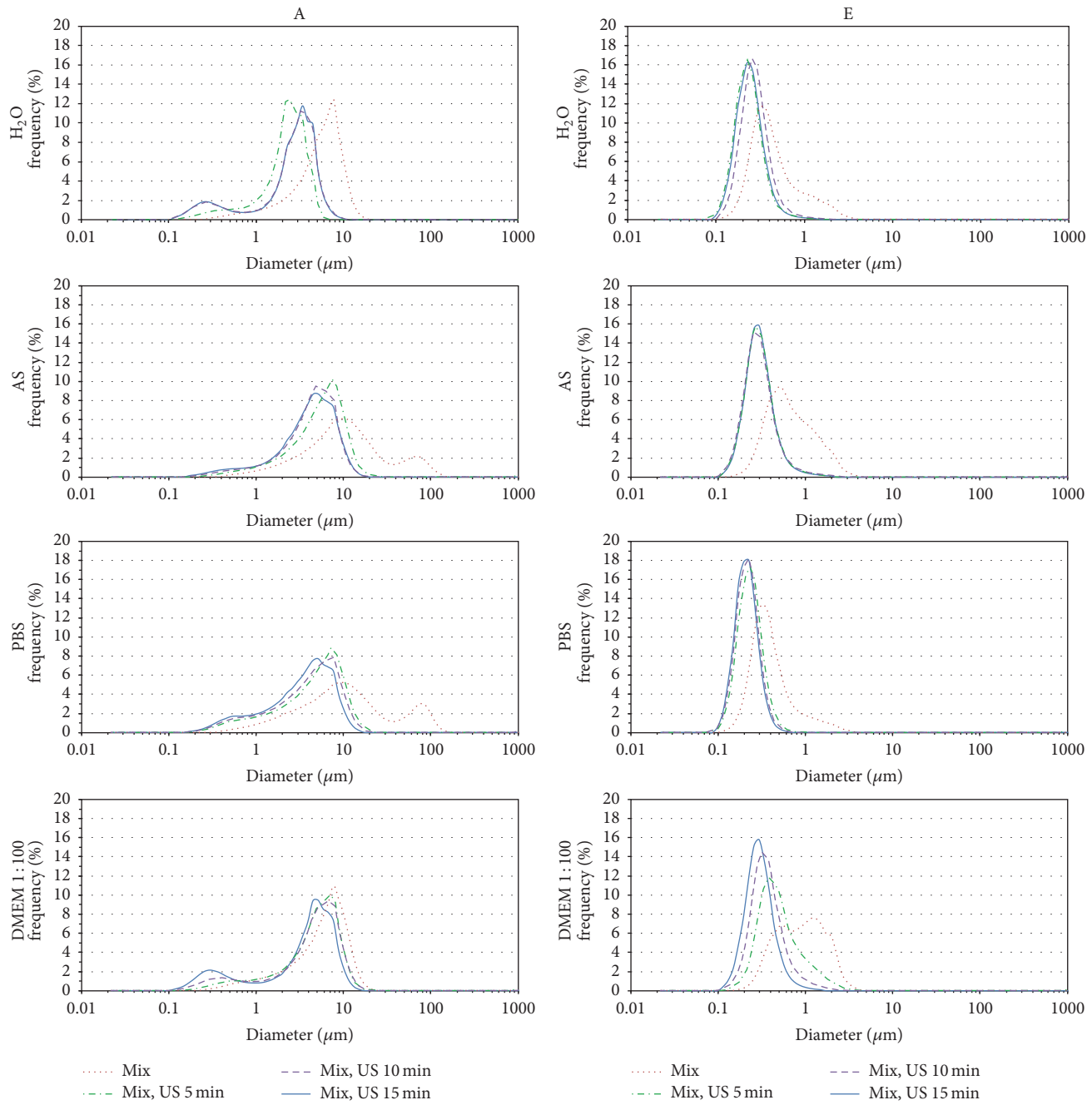

Figure 5: Multimodal particle size distribution (mix, red, dotted; mix + US 5 min, green, dash and dot; mix + US 10 min, violet, dashed; mix + US 15 min, blue, solid) for chewing gums A–E in different fluids: ultrapure water (H_2O), artificial saliva (AS), phosphate buffered saline solution (PBS), and diluted Dulbecco's Modified Eagle Medium for cell cultures (DMEM 1 : 100). mix: 5 min stirring. US: ultrasonication.

case of 0.005 w/v% concentration of FG-ref and sample E-3, respectively.

4. Discussion

The debate about the safety of TiO_2 (nano)particles used as food colour additives is still open, alongside the uncertainty on the threshold amount for a harmless human intake. Hence, a lot of research has been already focused on the toxicological aspects and risk assessment of TiO_2. During the in vitro studies, pristine TiO_2 (nano)particles are very often used as such in contact with cells. However, this experimental setting does not clearly represent the actual situation during food consumption, where TiO_2 is admixed into complex food matrixes (such as sugar-coated confectionery) as whitening additive.

Aware of that, the study design comprised two main parts and aimed to mimic the conditions of particles before their ingestion (i.e., mouth environment) and after ingestion (i.e.,

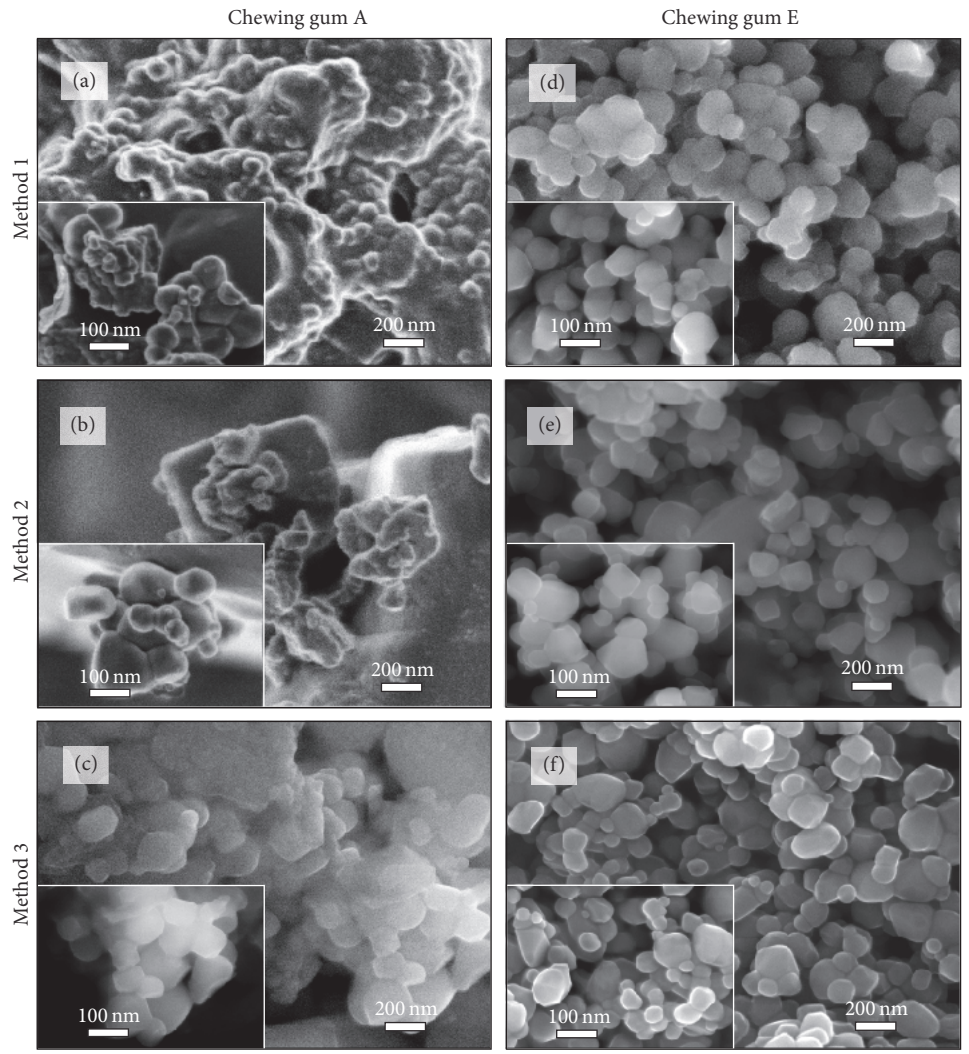

Figure 6: SEM of extracted particles from the coating of chewing gum: (a–c) A and (d–f) E.

stomach digestion), represented by "Step 1" and "Step 2" in Figure 1. Accordingly, "Step 1" analyses were deliberately performed on suspensions made of TiO_2 particles surrounded by the outer shell components (chewing gum "scraped" coating). This study approach is surely more valuable for simulating the actual events happening during chewing gum consumption. In fact, the hard, brittle sugary-based coating of chewing gums is crushed during the first bites to the pellet, and it is mostly swallowed as such, before it can get incorporated within the softer and sticky inner gum-based matrix. Chen et al. [13] measured that up to 95% of TiO_2 was swallowed by volunteering consumers in 10 min chewing. This event is applicable to any other confectionery product (e.g., candies or tablets). In view of that, the "scraped" and crushed coatings containing the TiO_2 particles were specifically analyzed in terms of stability/dispersion in various biologically relevant solvents during "Step 1."

4.1. Mimicking the Preingestion Phase (Step 1): "As-Scraped" Coatings as Colloids. Firstly, the prepared suspensions were characterised in terms of pH. The measurements were performed without any adjustment but at inherent pH, not to alter the conditions of the samples as such (Table 1). The different pHs in water can be ascribed to the presence of the other organic and inorganic ingredients of the sugar-based shell which embed the titania particles and screen them from the electrolyte. The buffer capacity of PBS and DMEM 1 : 1 kept the pH of suspensions almost constant, while no such effect occurred in artificial saliva (AS) or DMEM 1 : 100 (too diluted), so that the pH rose for all the samples.

Particle surface charge was assessed via zeta potential (ZP) measurements at inherent pH. The results indicate that all the "scraped" particles are negatively charged and, in general, display similar zeta potential in the same fluid (Figure 3(a)), with some exceptions attributable to the unpredictable effect of dissolved/undissolved gum ingredients on the ZP of the TiO_2 particles. The ZP measured for FG-ref in ultrapure water can be considered the actual ZP of food-grade titania. FG-ref displayed −37.5 mV for surface charge at inherent pH (6.7) in water, typical of a dispersed suspension.

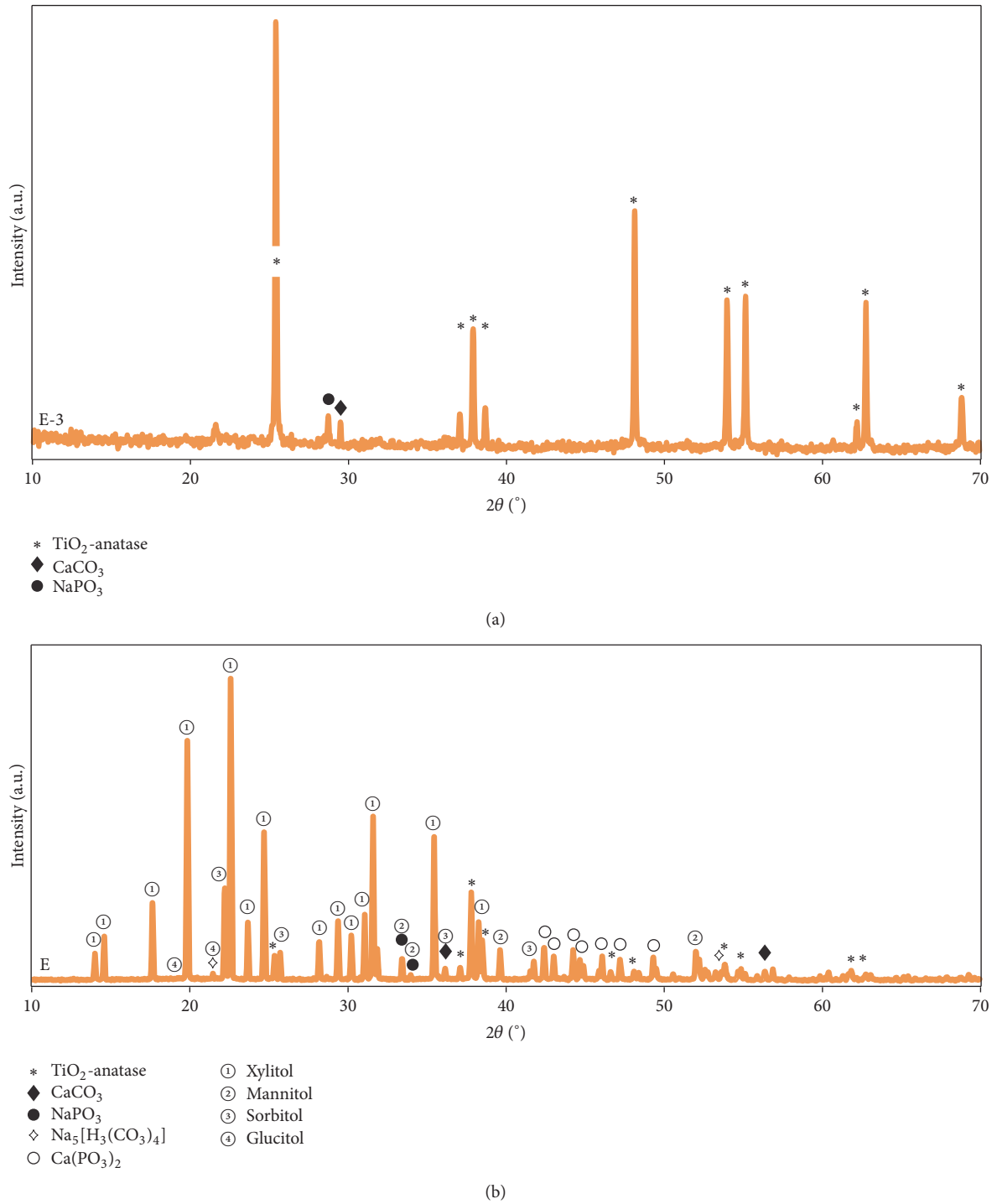

Figure 7: XRD diffractograms of chewing gum E: (a) particles E-3 extracted by Method 3; (b) "as-scraped" coating.

The FG-ref ability of forming well-dispersed suspensions justifies the reason of its spread use as artificial colorant for food preparations. In comparison to the bare FG-ref powder, the ZP decreased in magnitude (around −25 mV) for the sugar-based "scraped" coatings (samples A–E) dispersed in water. Even though this range is still considered applicable for moderately dispersed suspensions, this behaviour lets us assume that water is able to dissolve the sugar-based shell components quite efficiently so that the ions transferred in solution rose significantly the ionic strength of the solution. In general, high ionic strength and presence of multivalent ions in the electrolyte cause a tremendous shrinkage of the double layer around the particles. It can be estimated that the double layer thickness decreases down to ~1 nm for

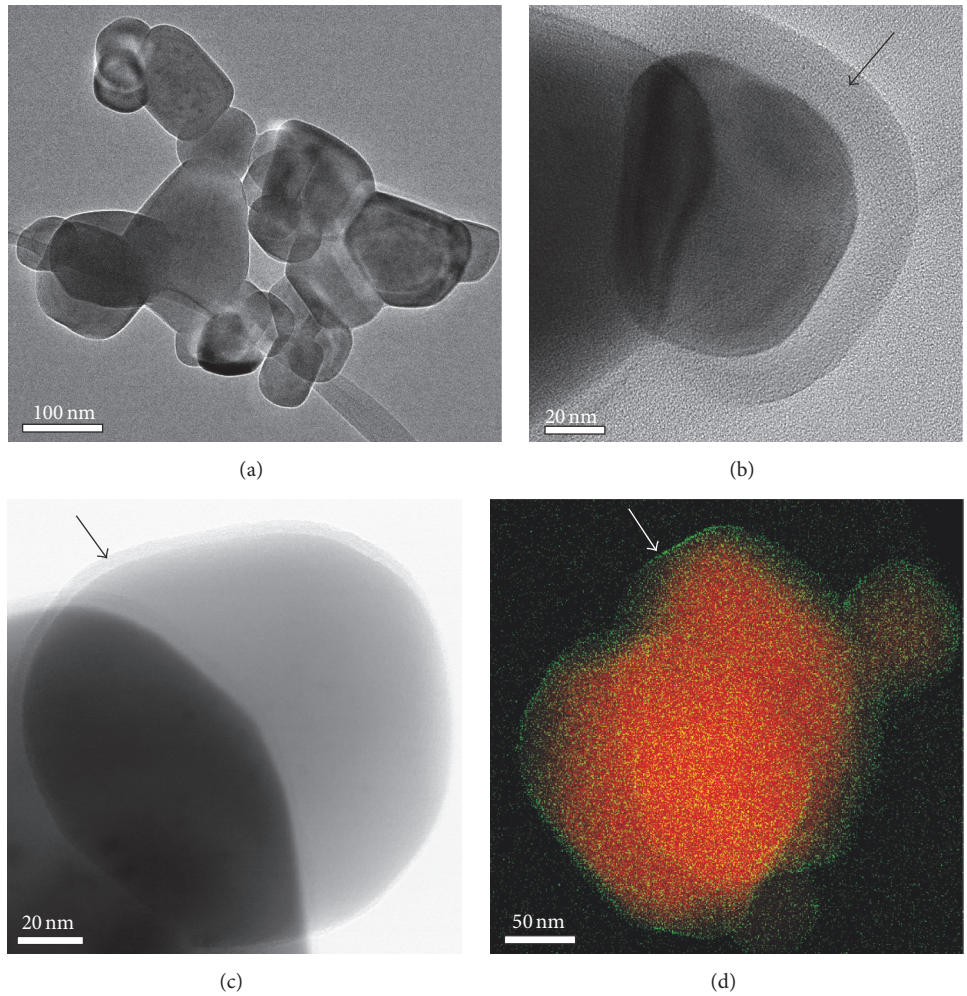

Figure 8: TEM images of (a) anatase nanoparticles aggregates from (b) FG-ref and (c) E-3 sample, decorated with the amorphous surface layer (indicated by arrows). (d) The elemental map of the anatase nanoparticle reveals the enrichment of surface layers by Si (Si: green, Ti: red).

multivalent ions and electrolytic concentrations ~0.2 M. As a consequence, the repulsive forces among the dispersed particles decreases and a strong particle agglomeration occurs. Accordingly, the surface charge of the particles composing the "scraped" triturate changed in magnitude by varying the solvent (mono- or multivalent ions) and the electrolytic concentration (ionic strength) (Figure 3(a)). For instance, the suspensions appeared quite unstable in artificial saliva and the ZP values dropped down to −10/−15 mV. In case of artificial saliva (AS), the solution contained urea, a carbamide presenting two amino groups joined by one carbonyl group. This molecule is able to form hydrogen bonds and acquires a positive net charge in aqueous solutions. Therefore, it is very likely that it serves as "bridge" between the negatively charged TiO_2 particles, enhancing the instability of the suspension. Different behaviour can be observed in PBS. FG-ref appeared quite dispersed, showing a surface charge of about −35 mV at physiological pH. In this case it can be assumed that the multivalent phosphate anions present in solution repel the TiO_2 particles (also negatively charged), so that the double layer is extended and the particles result more dispersed. The ZP was measured around −25 mV for the "scraped" chewing gum coatings; we believe that the buffering capacity of PBS somehow neutralised the effect of the dissolved ingredients from the coating. Similar behaviour to water was observed for suspensions in DMEM 1 : 100 medium, for which the copious dilution minimised the effect of the ionic strength. However, as for ultrapure water, this scenario does not represent the physiological ionic strength of body fluids. In fact, the effect of the electrolyte ionic concentration is evident when comparing the ZP values in DMEM 1 : 100 and DMEM 1 : 1, which shifted from about −30 mV (dispersed suspensions) in average to about −15 mV (agglomerated colloidal suspensions), similar to the values in AS. The competition among the multivalent ions contained in DMEM (phosphate, sulphate, calcium, and magnesium multivalent ions) had a drastic effect on abolishing the repulsion forces among the particles, destabilising the system. Moreover, the instability could have been enhanced also by the presence of various aminoacids dispersed in the medium, which could form a

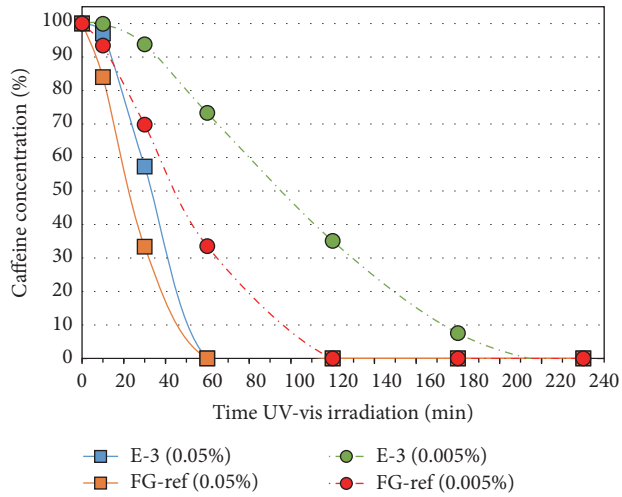

FIGURE 9: Caffeine degradation by TiO_2 food-grade powder (FG-ref) and extracted particles from chewing gum E (E-3) at two concentrations (0.05 w/v% and 0.005 w/v%) as a function of irradiation time.

corona around the particles and add interparticle interactions (meaning an enhancement of agglomeration).

The results on surface charge and colloidal stability reflected to the particle size distribution. Dynamic light scattering (DLS) calculates the distribution on an intensity basis; in this study DLS was used for obtaining the polydispersity index (PDI), representing the distribution width, and the effective diameter (D_{eff}) (Figure 3(b)). PDI was larger than 0.08 for all the samples, indicating a broad or polydisperse particle size distribution (as specified in the instruction manual of the instrument). In agreement with the surface charge results, the particles in H_2O and in DMEM 1 : 100 appeared well dispersed and presented small D_{eff} values, followed by the ones dispersed in PBS and AS (Figure 3(b)). For instance, in water the samples presented good dispersibility and the D_{eff} values of the agglomerates ranged between 200 and 300 nm (exception: chewing gum A). Therefore, it appears that the dissolved ingredients did not drastically destabilise the TiO_2 particles in suspensions, as revealed by the zeta potential data. The samples presented large scattering of data in case of physiological AS and PBS. At this point, one disadvantage of DLS technique has to be mentioned. Namely, the D_{eff} values could be overestimated, since the scattering effect produced by small particles could have been partially "hidden" by the scattering from big particles, the latter weighting the most in calculations.

Once the particles get in contact with the body fluids in vivo, they immediately interact with the present proteins by a dynamic process of association and dissociation, with the formation of a "nanoparticle-protein corona" around the particles as a final step [15]. It has been shown [11, 16] that such protein bonding affects the suspension stability of nanomaterials. Accordingly, the effect of a model protein (BSA) on the agglomeration state of the scraped coatings was also studied by DLS (Figure 4). The presence of BSA enhanced the dispersion of the particles, consistently with [11, 16], by diminishing the D_{eff} values for both materials, though in a different way (lowest D_{eff}: chewing gum E = 0.20 mg/mL BSA, FG-ref = 1.00 mg/mL BSA). As common for any surfactant, D_{eff} shows a parabolic trend, reaching a minimum at a certain BSA concentration before rising again. Indeed, surprisingly the pristine FG-ref powder presented higher D_{eff} values than chewing gum E scraped coating for all BSA concentrations, with initial coarse agglomerates of ~550 nm. In view of that, the higher dispersibility of TiO_2 particles embedded into the chewing gum matrix (scraped coating), improved in the presence of proteins like albumin, has to be taken into account for in vivo evaluations.

In order to study the size distribution of the "scraped" particles, laser diffraction (LD) was used as additional technique to DLS. The LD method applies the Mie scattering principle to assess calculations on volume-based particle distribution. When only stirring was applied prior analysis by LD (Figure 5, red dotted lines), the suspensions showed the same distribution trend as that by DLS analysis; therefore, the considerations previously done about the effect of the solvent composition and ionic strength on the particle distribution can be applied to the LD data as well. However, in terms of values, LD recorded higher particle dimensions than DLS. From the technical viewpoint, it can be supposed that DLS measured only the agglomerates sufficiently small and light to undergo electrophoretic mobility under the applied electric field, while the largest agglomerates, sedimented during the measurements in static conditions, were excluded from the calculations. Nevertheless, as already observed by DLS, laser diffraction results revealed a certain population fraction in the nanorange in all the applied conditions and especially after ultrasonication of the suspensions. Also, the formulation of the chewing gums seemed to account for the size distribution profiles (i.e., chewing gum A versus E in Figure 5).

Overall, the particle size results obtained with both DLS and LD techniques had the same trend in all the chosen media with comparable values. Moreover, the higher dispersibility reached in the presence of BSA deserves attention. In general, the particle size distribution data correlate well with the surface charge data: a low particle size and narrow distribution corresponded to nicely dispersible colloidal systems. Even though some of the particle size distribution value may seem too high to produce any harm or risk for health, Teubl et al. [9] reported that also submicron agglomerates (up to 400 nm) can penetrate, for instance, the buccal mucosa, and be internalised by buccal superficial cells into the human body. Hence, all the findings obtained by DLS, LD, and BSA addition have to be wisely considered prior any biological test.

4.2. Mimicking the Postingestion Phase (Step 2): Analyses on TiO_2 Extracted Particles. Once the scraped coating is swallowed, the ingredients undergo the main digestive phase. Accordingly, an extraction step was essential to separate and further characterise the (nano)particles. The extraction occurred by sequential dissolution, separation, and purification, according to three slightly different methods (Figure 2). The first step occurred in water to allow the dissolution of the sugary components. Centrifugation was chosen as

a simple and cost-effective method for particle separation without altering particle size or shape [13, 17], even though more sophisticated analytical techniques are known to be very effective for particle extraction and separation (i.e., microwave digestion, dry ashing, field flow fractionation, inductively coupled plasma spectrometry, and so on). Lastly, the purification occurred in water, ethanol, and acetone, avoiding any highly hazardous or environmentally risky chemical (e.g., strong acids).

The first investigation about the obtained powders aimed at the primary particle morphology and size by electron microscopy. All the extracted particles (samples A–E) had a round shape (Figure 6), with a primary particle size of in the range 130–150 nm. These data are in agreement with the primary particle size observed for TiO_2 particles previously found in food [6, 18] and our FG-ref reference powder. It has to be stressed at this point that none of the labels reported about the presence of "nano"ingredients on the label, even though 17–30% of the particles had dimensions below 100 nm, similarly to what was reported elsewhere [18].

The XRD analysis revealed that the all the extracted particles consisted of the anatase polymorph of TiO_2 (Figure 7(a)). This finding might be noticeable from the toxicological point of view, since it was suggested that the toxicity of TiO_2 nanoparticles depends also on their crystalline polymorph [19, 20], even though it has not been definitively confirmed yet. Even though the particles appeared very much clean in comparison to the original "scraped" powder (Figure 7(b)), the diffractograms show also the presence of calcium carbonate and sodium phosphate as residues after extraction by any method, so that the application of more effective techniques like (microwave-assisted) digestion in acids, dry ashing, or combustion is still preferable for a complete purification of the particles. Alternative extraction techniques would be particularly relevant for the samples A, B, and C, which presented low cleanness of the extracted particles (showing the most intense XRD peaks assigned to other residues besides TiO_2 (Figure S4), in agreement with the SEM images (Figures S1–3)) and, therefore, less effectiveness of the extraction methods in comparison to samples D and E. However, XRD could not reveal the nanometric, amorphous SiO_2 layer around the particles, which was identified indeed by high resolution TEM and EDXS elemental mapping (Figure 8).

Since most of the TiO_2 NPs used in commercialized products are surface modified to avoid any photocatalytic effect [21], we verified the potential photoactivity of the extracted particles enriched with SiO_2. In this regard, organics degradation under UV light is one of the most commonly used methods. Caffeine revealed to be a good organic model to verify the photoactivity of TiO_2 [12, 22]. Surprisingly, the experiments revealed that both TiO_2 particles E-3 and FG-ref were able to disrupt caffeine molecules under of UV irradiation (Figure 9), even at very low concentration (0.005 w/v%). The powders were revealed to be actually very photoactive, resulting in the total caffeine degradation after 1 h irradiation for 0.05 w/v% TiO_2 concentration, despite the presence of the SiO_2 amorphous coating. On the basis of this, an attempt to link the surface structure and chemistry observed by TEM with the physical and photoactivity properties can be made. It has been already shown that binary oxides SiO_2/TiO_2 show enhanced photocatalytic performances in comparison to bare TiO_2, which are attributable to several reasons, that is, the higher acidity of the surface hydroxyl groups of binary oxide systems [23] and the presence of a mixed TiOSi phase at the TiO_2/SiO_2 interface region [24]. In addition, our results indicate that the TiO_2 (nano)particles present in the chewing gums retain their catalytic power under UV irradiation even after processing (chewing gum production) and isolation (particle extraction). This finding can have an impact from the biological point of view. Sayes et al. [25] observed that nano-TiO_2 which acted as good photocatalysts were also the most cytotoxic and inflammatory-inducing in in vitro experiments. Moreover, the study described also the ability of nano-TiO_2 to produce reactive species under a wide range of conditions, even in the absence of light [25]. The authors suggested that Ti-OH anatase surfaces, in the presence of appropriate donors, may be reactive enough to oxidatively damage biological species also without light exposure [25]. Another study reported about the radical reactions occurring at the surface of fine and ultrafine TiO_2 regardless of UV irradiation [26]. Also, anatase was reported to react towards organic molecules via cleavage of their C-H bonds in dark conditions [26]. Besides, it has been found that other nanoparticles may be affected by the conditions of the digestive track, becoming very reactive and toxic [27–29]. In view of that, cellular toxicity and inflammation derived by the titania ability to generate radical species may be worth of deeper biological investigations.

5. Conclusions

This research highlights hidden aspects of food-grade TiO_2 characteristics, when the particles operate in their real environment. The size distribution of particles contained in the scraped coatings appeared close to the nanorange in suspension in water and simulated body fluids. All the samples showed negative surface charge, though with different ZP magnitude and degree of dispersion according to the different electrolytic solutions. The ZP became sufficiently low in presence of albumin, which acted as a surfactant and promoted the dispersion of the scraped coatings.

Simple methods were applied to extract the particles from the chewing gum matrix, namely, steps of dissolution (ultrasonication), separation (centrifugation), and purification (various organic solvents). SEM observations confirmed that the mean size of the extracted particles was close to the nanorange (~130 nm), with a 17–30% of them having dimensions below 100 nm. Also, the presence of undeclared amorphous SiO_2 in the outer shell, revealed by TEM, did not hinder the photocatalytic activity of the extracted particles. Such photoinduced phenomenon may account for undesired in vivo radical reactions.

Taken as a whole, depending on the composition of the chewing gums from different brands, the extraction methods and sample preparation (i.e., mixing, ultrasonication) used in this study resulted in distinctive effects on the behaviour of the TiO_2 (nano)particles, that is, their cleanness after extraction, their colloidal stability, and particle size, and so

on. This may suggest a different ability of the coating to release the TiO_2 in an aqueous environment (like the body fluids) and may account for a diverse behaviour of the chewing gums during their consumption.

Conflicts of Interest

The authors declare that they have no conflicts of interest.

Acknowledgments

Funding by the European Commission within the framework of the "ISO-FOOD ERA Chair for Isotope Techniques in Food Quality, Safety and Traceability" project (FP7-REGPOT no. 621329) is acknowledged. The authors wish to thank Bojan Ambrožič for his help with TEM imaging.

References

[1] European Parliament and Council, "Council Regulation (EC) No 1331/2008 of the European Parliament and of the Council of 16 December 2008 establishing a common authorisation procedure for food additives, food enzymes and food flavourings," *Official Journal of the European Union*, vol. L354, no. 51, pp. 1–6, 2008.

[2] European Commission, "European Parliament and Council Directive 94/36/EC of 30 June 1994 on colours in foodstuffs," *Official Journal of the European Communities*, vol. L237, no. 37, pp. 13–29, 1994.

[3] European Parliament and Council, "Annex II to Regulation (EC) No 1333/2008 of the European Parliament and of the Council by establishing a Union list of food additives," *Official Journal of the European Union*, vol. L354, 2008.

[4] Food and Drug Administration, "Food and Drugs, revised as of April 1, 2015," *Code of Federal Regulations*, vol. 1, pp. 1–99, 2015.

[5] European Commission, "Commission Recommendation 2011/696/EU of 18 October 2011 on the definition of nanomaterial," *Official Journal of the European Union*, vol. L275, no. 54, pp. 38–40, 2011.

[6] A. Weir, P. Westerhoff, L. Fabricius, K. Hristovski, and N. Von Goetz, "Titanium dioxide nanoparticles in food and personal care products," *Environmental Science and Technology*, vol. 46, no. 4, pp. 2242–2250, 2012.

[7] "Guidance on the risk assessment of the application of nanoscience and nanotechnologies in the food and feed chain," *EFSA Journal*, vol. 9, no. 5, 2011.

[8] E. Fröhlich, "The role of surface charge in cellular uptake and cytotoxicity of medical nanoparticles," *International Journal of Nanomedicine*, vol. 7, pp. 5577–5591, 2012.

[9] B. J. Teubl, G. Leitinger, M. Schneider et al., "The buccal mucosa as a route for TiO_2 nanoparticle uptake," *Nanotoxicology*, vol. 9, no. 2, pp. 253–261, 2014.

[10] K. J. Knutson and D. W. Berzins, "Corrosion of orthodontic temporary anchorage devices," *The European Journal of Orthodontics*, vol. 35, no. 4, pp. 500–506, 2013.

[11] P. Bihari, M. Vippola, S. Schultes et al., "Optimized dispersion of nanoparticles for biological in vitro and in vivo studies," *Particle and Fibre Toxicology*, vol. 5, article no. 14, 2008.

[12] M. Lorenzetti, D. Biglino, S. Novak, and S. Kobe, "Photoinduced properties of nanocrystalline TiO_2-anatase coating on Ti-based bone implants," *Materials Science and Engineering C*, vol. 37, pp. 390–398, 2014.

[13] X.-X. Chen, B. Cheng, Y.-X. Yang et al., "Characterization and preliminary toxicity assay of nano-titanium dioxide additive in sugar-coated chewing gum," *Small*, vol. 9, no. 9-10, pp. 1765–1774, 2013.

[14] J. Athinarayanan, A. A. Alshatwi, V. S. Periasamy, and A. A. Al-Warthan, "Identification of nanoscale ingredients in commercial food products and their induction of mitochondrially mediated cytotoxic effects on human mesenchymal stem cells," *Journal of Food Science*, vol. 80, no. 2, pp. N459–N464, 2015.

[15] I. Lynch and K. A. Dawson, "Protein-nanoparticle interactions," *Nano Today*, vol. 3, no. 1-2, pp. 40–47, 2008.

[16] R. C. Murdock, L. Braydich-Stolle, A. M. Schrand, J. J. Schlager, and S. M. Hussain, "Characterization of nanomaterial dispersion in solution prior to in vitro exposure using dynamic light scattering technique," *Toxicological Sciences*, vol. 101, no. 2, pp. 239–253, 2008.

[17] J.-H. Lim, P. Sisco, T. K. Mudalige, G. Sánchez-Pomales, P. C. Howard, and S. W. Linder, "Detection and characterization of SiO_2 and TiO_2 nanostructures in dietary supplements," *Journal of Agricultural and Food Chemistry*, vol. 63, no. 12, pp. 3144–3152, 2015.

[18] R. J. B. Peters, G. van Bemmel, Z. Herrera-Rivera et al., "Characterization of titanium dioxide nanoparticles in food products: analytical methods to define nanoparticles," *Journal of Agricultural and Food Chemistry*, vol. 62, no. 27, pp. 6285–6293, 2014.

[19] J. Wang, C. Chen, Y. Liu et al., "Potential neurological lesion after nasal instillation of TiO_2 nanoparticles in the anatase and rutile crystal phases," *Toxicology Letters*, vol. 183, no. 1-3, pp. 72–80, 2008.

[20] C. Jin, Y. Tang, F. G. Yang et al., "Cellular toxicity of TiO_2 nanoparticles in anatase and rutile crystal phase," *Biological Trace Element Research*, vol. 141, no. 1-3, pp. 3–15, 2011.

[21] M. Fisichella, F. Berenguer, G. Steinmetz, M. Auffan, J. Rose, and O. Prat, "Intestinal toxicity evaluation of TiO_2 degraded surface-treated nanoparticles: a combined physico-chemical and toxicogenomics approach in caco-2 cells," *Particle and Fibre Toxicology*, vol. 9, no. 1, article 18, 13 pages, 2012.

[22] R. R. N. Marques, M. J. Sampaio, P. M. Carrapiço et al., "Photocatalytic degradation of caffeine: developing solutions for emerging pollutants," *Catalysis Today*, vol. 209, pp. 108–115, 2013.

[23] X. Fu, L. A. Clark, Q. Yang, and M. A. Anderson, "Enhanced photocatalytic performance of titania-based binary metal oxides: TiO_2/SiO_2 and TiO_2/ZrO_2," *Environmental Science and Technology*, vol. 30, no. 2, pp. 647–653, 1996.

[24] C. Anderson and A. J. Bard, "Improved photocatalytic activity and characterization of mixed TiO_2/SiO_2 and TiO_2/Al_2O_3 materials," *Journal of Physical Chemistry B*, vol. 101, no. 14, pp. 2611–2616, 1997.

[25] C. M. Sayes, R. Wahi, P. A. Kurian et al., "Correlating nanoscale titania structure with toxicity: a cytotoxicity and inflammatory response study with human dermal fibroblasts and human lung epithelial cells," *Toxicological Sciences*, vol. 92, no. 1, pp. 174–185, 2006.

[26] I. Fenoglio, B. Fubini, E. M. Ghibaudi, and F. Turci, "Multiple aspects of the interaction of biomacromolecules with inorganic surfaces," *Advanced Drug Delivery Reviews*, vol. 63, no. 13, pp. 1186–1209, 2011.

[27] L. Wang, D. K. Nagesha, S. Selvarasah, M. R. Dokmeci, and R. L. Carrier, "Toxicity of CdSe nanoparticles in Caco-2 cell cultures," *Journal of Nanobiotechnology*, vol. 6, article no. 11, 2008.

[28] H. Meng, Z. Chen, G. Xing et al., "Ultrahigh reactivity provokes nanotoxicity: explanation of oral toxicity of nano-copper particles," *Toxicology Letters*, vol. 175, no. 1-3, pp. 102–110, 2007.

[29] C. Corredor, M. D. Borysiak, J. Wolfer, P. Westerhoff, and J. D. Posner, "Colorimetric detection of catalytic reactivity of nanoparticles in complex matrices," *Environmental Science & Technology*, vol. 49, no. 6, pp. 3611–3618, 2015.